https://doi.org/10.1016/j.jclepro.2017.10.347

Wind resource potential assessment using a long term tower measurement approach: A case study of Beijing in China

Liu Junkai [a,b]; Gao Chloe Y. [c]; Ren Jingzhen [e]; Gao Zhiqiu [a,d *]; Liang Hanwei [d]; Wang Linlin [a]

a State Key Laboratory of Atmospheric Boundary Layer Physics and Atmospheric Chemistry (LAPC), Institute of Atmospheric Physics, Chinese Academy of Sciences, Beijing 100029, China

b University of Chinese Academy of Sciences, Beijing 100049, China

c Department of Earth and Environmental Sciences, Columbia University, New York, NY 10027, USA

d Collaborative Innovation Center on Forecast and Evaluation of Meteorological Disasters, School of Geography and Remote Sensing, Nanjing University of Information Science & Technology, Nanjing, 210044, China

e Department of Industrial and Systems Engineering, The Hong Kong Polytechnic University, Hong Kong SAR, China

* Corresponding author. E-mail address: zgao@mail.iap.ac.cn (Z. Gao).

Abstract

With exacerbating air quality due to pollutant emissions and rising energy supply crisis, the wind energy consumption will play a key role in future energy structure in China. To utilize the wind energy optimally, a better understanding and quantification of wind resource such as the temporal-spatial and vertical distributions is vital prior to exploitation. Based on wind measurements from 1991 to 2011 on a 15-level 325 m meteorological tower in Beijing, we assessed the potential of wind resource using the Weibull function and the wind atlas analysis and application program (WAsP) software. Results show that wind resource has significant seasonal and diurnal variations and diurnal variation varies with height. Additionally, although the wind resource increases with height, there is a strong wind shear layer related to the complex urban underlying surface. Furthermore, observation and WAsP simulation show that larger wind resource mainly comes from northwest wind in northwestern or northern Beijing. However, considering the regional average wind resource, we concluded that wind resource in Beijing is suitable for small wind turbines, yet the decreasing trends of wind resources seem to make wind energy unsustainable.

Keywords: Wind speed; Wind power density; Weibull function; WAsP model

1. Introduction

The International Energy Agency aims to deal with the conventional energy supply crisis and its negative effects through alternative energy in this century, and it is estimated that there would be more than $38 trillion of new energy infrastructure

construction by 2035 (IEA, 2011). Among these new energy sources, wind energy, as a clean and renewable energy, has been developed rapidly in many countries (Martin, 2010). In 2012, China surpassed the United States to become the fastest growing wind energy market in the world (Zeng et al., 2013).

Past studies about wind resource in China have mainly focused on the northeast and northwest of China, coastal zones of East China Sea, and South China Sea (e.g., Zhou et al., 2011, Zheng et al., 2012, Wu et al., 2013). However, as a typical inland city, Beijing has been suffering from exacerbating environmental and energy issues associated with the rapid expansion of population in recent years. As a result, wind energy demand in great cities has become more urgent (Stankovic, 2009). At the same time, to avoid a high economic cost and technological stress from long-distance energy transportation project, the development of the miniaturization and industrialization of wind turbines makes the exploitation of wind resource in local urban or pre-urban area become more feasible (Walker, 2011, Ishugah et al., 2014, Wang and Teah, 2017), which has drawn growing interest from researchers (e.g., Grant et al., 2008, Albadi et al., 2009, Walker, 2011, Ishugah et al., 2014, Laiola and Giungato, 2017). Thus, a more accurate assessment of wind resource in Beijing is greatly needed.

Preliminary evaluation of wind resource is of vital importance for the exploitation and utilization of wind energy. To date, there are two popular methods for estimating wind resource: one is based on the output data from numerical models (e.g., WRF and MM5) (Jimenez et al., 2007), and another is based on the data from meteorological

stations (Belu and Koracin, 2009). However, both of the two traditional methods have some disadvantages when they are adopted for different purposes. The former method, which uses high-resolution data from mesoscale numerical models, is not only weak in handling smaller scale phenomena, but also creates operational difficulties in wind energy industry due to a large amount of calculation resource and time (Fang, 2014). Therefore, there is an urgent need for a wind resource assessment method with high resolution using only a few meteorological stations or towers in larger areas. At present, several kinds of softwares were developed by commercial companies through simplifying numerical models according to different assumptions. In particular, the WAsP developed by the Danish Riso National Laboratory (DRNL) has become the standard tool for wind resource assessment in the wind energy industry (DTU, 2016), and it has been successfully used to conduct wind resource assessments (e.g., Boehme and Wallace, 2008, Ko et al., 2009, Fang, 2014). The errors from WAsP are usually less than 10% (Bechrakis et al., 2004, Ko et al., 2009, Fang, 2014). Even with data from just one meteorological station or tower, WAsP is still able to provide satisfactory results. On the other hand, since the distribution of meteorological stations is sparse, it is unable to provide wind resource assessment with high resolution using data from these stations. Moreover, these wind observations mainly focus on the 10-m height, there is a lack of wind data at high levels, which limits the exploitation of wind resource at upper levels. Even the models have outputs of multi-level wind data, the forecast data are not accurate and the heights of wind data from models usually focus on above 100 m. Considering that the heights of wind turbines usually vary from 20 m to 120 m, the

wind data within near surface layer also needs to be interpolated by log-law or power-law. Also, the lack of wind data at high levels limits the estimation and understanding of wind shear or wind stress at upper levels, which influences the safety of wind turbines greatly. Furthermore, if there is a high safety risk of wind turbines with strong wind shear or wind stress, the height or location with rich wind resource is still unsuitable for exploitation. Therefore, the multi-layer wind observation data could provide a good opportunity to investigate the vertical variations of wind shear and reduce the wind resource assessment error induced by the vertical interpolation based on the data from meteorological stations or models. Nfaoui et al. (1998) further pointed out that the length of observational data was crucial to the assessment result - at least 10 years of observation data is need to get a more accurate result. Longer time series of data also has less potential for errors than shorter time series does. Therefore, the data of a 325 m meteorological tower located in the center of Beijing (39.97 N, 116.37 E, 48.63 m above sea level) provides a good condition to assess the wind resource in this large city, especially since the instruments for measuring wind installed at multiple layers on this tower have been in operation for nearly 30 years without any migration. More importantly, the data collected from this tower is continuous and reliable since the tower's establishment in 1978. Long-term data collected from this tower has become one of the most important datasets used to analyze urban wind (e.g., Li et al., 2010, Wang et al., 2014).

Due to the lack of long time scale data from tall towers, most of the past studies were based on data from standard non-tower meteorological stations or model output,

whereas studies of wind resource in large cities using the tower data with high precision and high resolution rarely exist. Therefore, based on the multi-layer observation data of a single meteorological tower in city, not only can we investigate the temporal, azimuthal and vertical distributions of wind resources, but we can also use WAsP to study spatial distribution of wind resource at higher resolutions.

In this study, the available and high-quality wind data from a multi-layer meteorological tower in Beijing, along with the terrain data from Shuttle Radar Terrain Mission (STRM) and the roughness length information of different underlying surfaces is used to conduct this research using the Weibull function and the WAsP software. This paper was organized as follows: annual and diurnal variations, wind rose, vertical distribution, comparison between simulation and observation, spatial distribution with high resolution and trend of wind resource. The objective of this paper is to assess the condition of wind resource and provide recommendations for the wind energy industry in Beijing.

2. Data and methods

As mentioned previously, the quality of wind data and the calculation of wind power are important factors for wind resource assessment. In this section, we firstly presented the long-term observation data at multiple layers, and then we used different methods as follows to analyze the various characteristics of wind resource.

2.1. Data

The meteorological data used in this study were collected at 15 levels (i.e., 8 m, 15 m, 32 m, 47 m, 63 m, 80 m, 106 m, 102 m, 120 m, 140 m, 160 m, 180 m, 200 m, 240 m, 280 m and 320 m) from a 325 m meteorological tower in Beijing during 1991–2011. In order to avoid the wake effect, the tower was built with an open structure, and slow-response observational instruments (e.g., anemometers, vanes) were installed on two booms of 4 m extending northwest and southeast from the tower, which are the prevailing wind directions. The sampling frequency of all instruments was 0.05 Hz, and the original data went through the following quality control prior to use: first, unrealistic data such as wind speeds outside of the range from 0 to 50 ms^{-1}, wind directions greater than 360° or lower than 0°, were excluded. Second, data spikes were corrected using the cubic interpolation function. In this paper, hourly-averaged wind data were used. Since the urban atmospheric boundary layer (UABL) can be divided into four sublayers, urban canopy, roughness sublayer, surface layer and mixed layer (Oke, 1988), the 325 m meteorological tower almost covers the whole UABL. Wang et al. (2014) considered that 47 m, 140 m and 280 m can be used as the representative height of roughness sublayer, surface layer, and mixed layer, respectively. Therefore, 15 m, 47 m, 140 m, and 280 m were selected to analyze the wind resource in Sections 3.1 Annual and diurnal variation patterns of wind resource, 3.2 Wind rose, 3.3 Comparison between Weibull function prediction and the measurements.

Topographic data of Beijing is an important input in the WAsP software. Therefore, STRM data with a resolution of 30 m from National Aeronautics and Space

Administration (NASA) were applied in this study, and the data were pretreated by the Consortium of International Agricultural Research Centers-the Consortium for Spatial Information (CGIAR-CSI) to filter out noise. The elevation of Beijing is between 0 m and 2283 m. In order to improve the reliability of the results from WAsP, we selected an elevation interval of 5 m for the contour lines in the flat area (<=100 m) and 50 m in steep area (>100 m). Due to the lack of roughness information with high resolution, the land surface in Beijing could be divided into four types: urban, suburban, water and forest, and the default roughness lengths in WAsP are 1.0, 0.5, 0 and 0.8 m, respectively. Consequently, these data would be processed by Map Editor of WAsP and Arcgis tools (Childs, 2004) to become a digital map.

2.2. Method

For the long-term data, it is computationally onerous to calculate the enormous hourly time-series wind data (Zhou et al., 2006). In order to reduce computation, we described the characteristics of a wide range of wind data using a distribution function with only a few key parameters. Compared to other statistical distribution functions (i.e., Log-normal and Rayleigh probability distributions), the Weibull function has been applied in many wind resource assessment studies, and it has better stable accuracy in analyzing and interpreting the actual wind speed data (e.g., Zhou et al., 2006, Koroneos et al., 2007, Keyhani et al., 2010, Fagbenle et al., 2011, Wu et al., 2013, Pishgar-Komleh et al., 2015). Meanwhile, compared to the mesoscale numerical model, the simplified WAsP model is more convenient and suitable for smaller scale study

considering limited computational resource and time (e.g., Boehme and Wallace, 2008, Ko et al., 2009, Fang, 2014), and it has been widely used in wind energy industry as mentioned above. Therefore, the Weibull function and WAsP model are used in this paper.

2.2.1. Weibull function

Th e probability density function of the Weibull is Equation (1).

$$f(v) = \left(\frac{k}{c}\right)\left(\frac{v}{c}\right)^{k-1} exp\left[-\left(\frac{v}{c}\right)\right]^{k} \tag{1}$$

The corresponding cumulative probability function of Weibull distribution is Equation (2).

$$F(v) = 1 - exp\left[-\left(\frac{v}{c}\right)^{k}\right] \tag{2}$$

where $f(v)$ is the probability of observing wind speed (v), $F(v)$ is the cumulative distribution function of observing wind speed (v), and c represents the scale parameter while k represents the dimensionless shape factor of the distribution.

k and c can be calculated by Equations (3), (4).

$$k = \left(\frac{\sigma}{v_{avg}}\right)^{-1.086} \tag{3}$$

$$c = \frac{v_{avg}}{\mathcal{T}(1-1/k)} \tag{4}$$

where v_{avg} and σ are the average and variance of wind speed. T is the Gamma function, which is expressed as:

$$\mathcal{T}(x) = \int_{0}^{\infty} e^{-u} u^{x-1} du \tag{5}$$

Accordingly, the mean wind speed (MWS) can be determined by Equation (6).

$$\mathrm{MWS} = \int_0^{\infty} v f(v)\, dv \tag{6}$$

The effective wind power density (EWPD) for wind turbines can be calculated by Equation (7).

$$\mathrm{EWPD} = \frac{1}{2} \int_{v_1}^{v_2} \rho v^3 f'(v)\, dv \tag{7}$$

where v_1 is the starting speed (3 m s^{-1}), v_2 is the cutting speed (25 m s^{-1}) and ρ is the air density (1.23 kg m^{-3}).

$f'(v)$in Equation (8) is the probability density function of the effective wind speed.

$$f'(v) = \frac{f(v)}{F(v_2) - F(v_1)} \tag{8}$$

Both MWS and EWPD are common indices for wind resource assessment. The wind power density can also be determined by Equation (9).

$$\mathrm{WPD} = \frac{1}{2} \int_0^{\infty} \rho v^3 f(v)\, dv. \tag{9}$$

2.2.2. WAsP model

The WAsP model applies several models to generalize a set of wind observational data into regionally representative wind climatology by modelling wind flow across the landscape. Once the statistics of model, derived from a set of long-term wind speed and direction data at a reference site, are obtained by fitting into a Weibull distribution, these outcomes are extrapolated by modelling the effects of obstacles, surface roughness and topography (Jimenez et al., 2007, Sveinbjornsson, 2013, DTU Wind Energy, 2016). In these models, the WAsP program is essentially based on the Jackson-

Hunt theory. It simplifies the Navier-Stokes equations according to several assumptions including a steady state flow, linear advection and first order turbulence closure (Truepower, 2010). Moreover, it hypothesizes that under a stable atmosphere, there is a balance between the pressure force and the Coriolis force in wind flows. Following these hypotheses and statistics, topography and surface roughness information surrounding the reference station can be used to calculate the geostrophic wind which is based on the geostrophic drag law. A logarithmic law of wind profile is also used to compute the change of wind speed with height in WAsP.

3. Results and discussion

3.1. Annual and diurnal variation patterns of wind resource

The monthly MWS and EWPD with similar patterns of variation at four levels are shown in Fig. 1. From March to May, the MWS and EWPD are relatively high, while their values become very small from July to September. The monthly maximums of MWS and EWPD occur in April and their minimums appear in August. Both MWS and EWPD increase initially and then decrease later in the year. The seasonal maximums of MWS and EWPD occur in spring and their minimums appear in summer (Table 1). This annual variation is due to Beijing's closer proximity to the wind source in spring and winter months. It is also a result of the difference in monsoon intensity in winter and summer, where the winter monsoon is stronger than the summer monsoon. The range of annual variation increases with height, which indicates that the wind resource are more stable at lower levels, yet the MWS and EWPD at lower levels are small year

round. Islam et al. (2011) pointed out that this condition might still be promising for small-scale wind turbine applications with technological development.

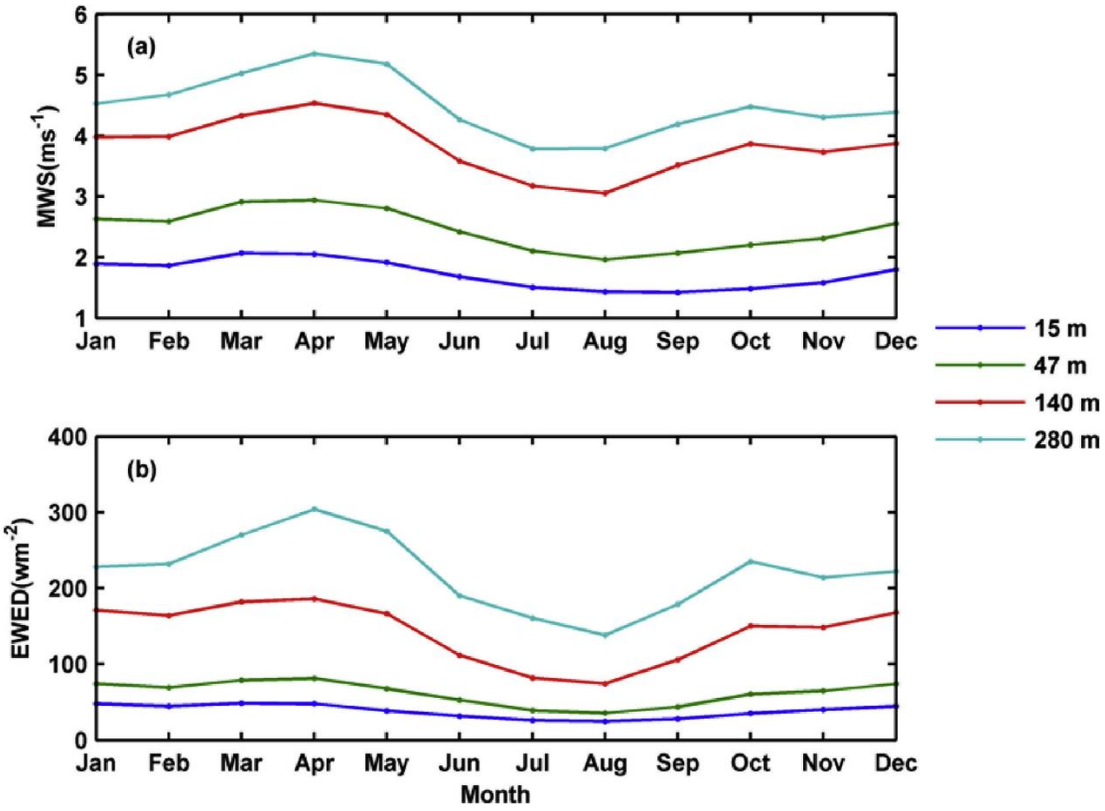

Fig. 1. The annual variation patterns of (a) wind speed and (b) effective wind power density at four levels in Beijing.

Table 1. The statistic results of MWS and EWPD.

Height (m)	MWS (ms^{-1})						EWPD (wm^{-2})					
	Spring	Summer	Autumn	Winter	Day (06–17)	Night (18–05)	Spring	Summer	Autumn	Winter	Day (06–17)	Night (18–05)
15	2.0	1.4	1.6	1.9	1.9	1.5	45	28	34	46	40	34
47	2.9	2.1	2.2	2.6	2.7	2.3	76	43	56	73	67	54
140	4.4	3.3	3.7	4.0	3.7	4.0	178	89	135	168	136	148
280	5.2	4.0	4.3	4.5	4.1	4.9	283	163	209	228	175	272

The diurnal variation patterns of MWS and EWPD are displayed in Fig. 2. The curves of diurnal variation at 15 m and 47 m show a single peak. The maximums of MWS and EWPD appear at 15:00. As a result of the strong thermal effect in the city, the MWS and EWPD in the daytime are larger than those in the nighttime (Table 1). Liu et al. (2013) also found similar diurnal variation of wind resource of 10 m at three other sites in China. On the contrary, the minimums of MWS and EWPD at 140 m and 280 m occur at 09:00 or 12:00, and the maximum values peak at 17:00 or 21:00. Wind resource in the nighttime is larger than that in the daytime (Table 1), this is because the nocturnal jet caused by large wind shear associated with the thermal inversion often happens in the nighttime, and the thermal effect seldom reaches higher levels in the daytime. Since the normal electrical energy demand in cities usually has two peaks in a day, one is often around noon in the daytime, the other is from dusk to midnight due to anthropogenic activities (BET, 2004, Bahaj et al., 2007). The occurrence times of peaks in diurnal demand almost match those of the maximums of MWS and EWPD at lower and higher levels. It would make wind energy utilization more efficient when supply and demand reaches equilibrium.

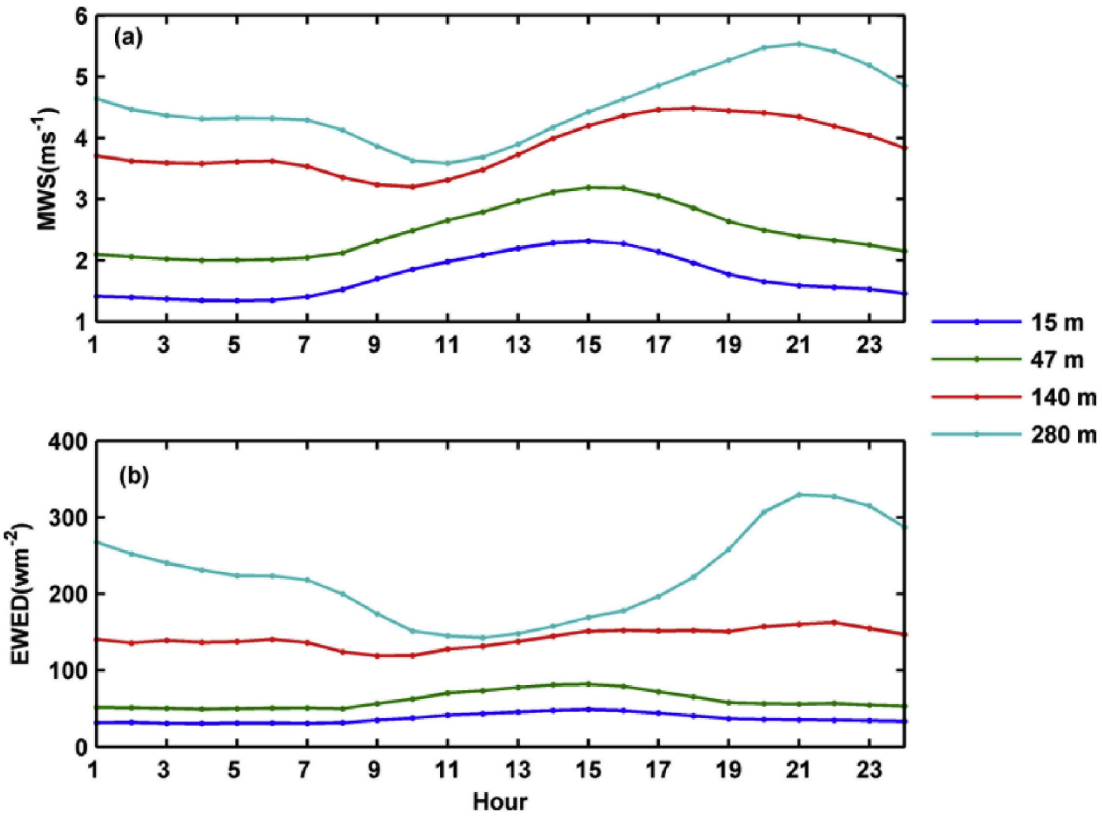

Fig. 2. The diurnal variation patterns of (a) wind speed and (b) effective wind power density at four levels in Beijing.

3.2. Wind rose

Considering the heterogeneity of the underlying surface and the variability of wind direction, the wind turbines need to face toward the optimal direction. The MWS and EWPD in different directions are shown in Fig. 3. The wind direction was equally classified into eight sectors (N, NE, E, SE, S, SW, W, NW) with the central degree of 0°, 45°, 90°, 135°, 180°, 225°, 270° and 315°, respectively. The MWS at 15 m and 47 m are relatively steady with a range of 0–1 m s^{-1}, and the maximum values appear in the W and NW sectors. Compared to the lower levels, the MWS at 140 m and 280 m have a wider range of 3 m s^{-1}, and the maximum values appear in

the N and NW sectors. The EWPD have similar variation as the MWS, and the maximum values are shown in the NW, W, and N sectors. Generally, the higher EWPD and MWS occur between the W sector and N sector, which indicate that the northwest wind could bring more wind resource to Beijing. Therefore, it is better for a wind turbine to face the NW sector.

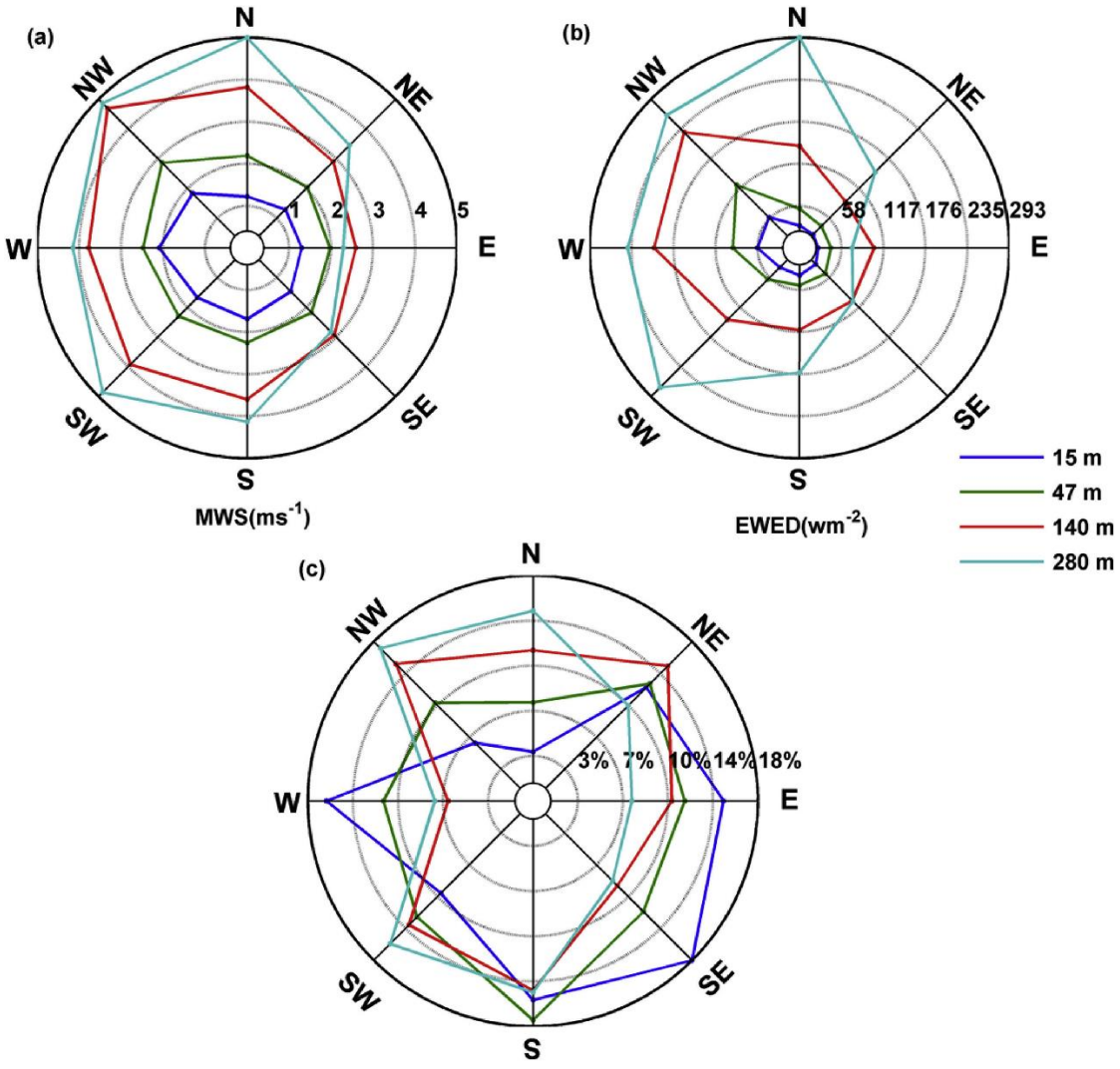

Fig. 3. The (a) wind speed, (b) effective wind power density and (c) wind direction roses at four levels in Beijing.

The statistical results of the frequencies of wind direction in the eight sectors are

also displayed in Fig. 3c. The distributions of wind direction show various roses at different levels. The northwest wind has the maximum percentages of 17% at 140 m or 15% at 280 m. The frequency of north wind is evidently greater than that of the south wind shown in the figure. It is also reflected by the MWS and EWPD roses that the northern sectors have more wind resource. However, the inverse conditions are shown at 15 m and 47 m. Although the south wind emerges more frequently in Beijing, the MWS and EWPD roses fail to reveal this condition, for the strength of the south wind is relatively weaker than that of the north wind. It implies that for the selection of optimal direction, both the strength of wind speed and the frequency of winds from different directions should be considered.

3.3. Comparison between Weibull function prediction and the measurements

The Weibull function and the wind speed and wind power density distributions, calculated from the available wind data at four levels during 1991–2011, are presented in Fig. 4, where the wind speed interval is 1 m s-1. In Fig. 4, the evaluation criteria of how close the probability predicted by Weibull distribution is to the frequency obtained from the actual wind speed data, is used to assess the accuracy of the Weibull function (Zhou et al., 2006). It is indicated previously in Persaud et al. (1999) that Weibull function does not simulate well the lower wind speed close to zero. However, for the purpose of the EWPD assessment, the discrepancy below wind speed of 3 m s-1 may be ignored, since the Weibull function could describe the wind data well in the range of effective wind speed.

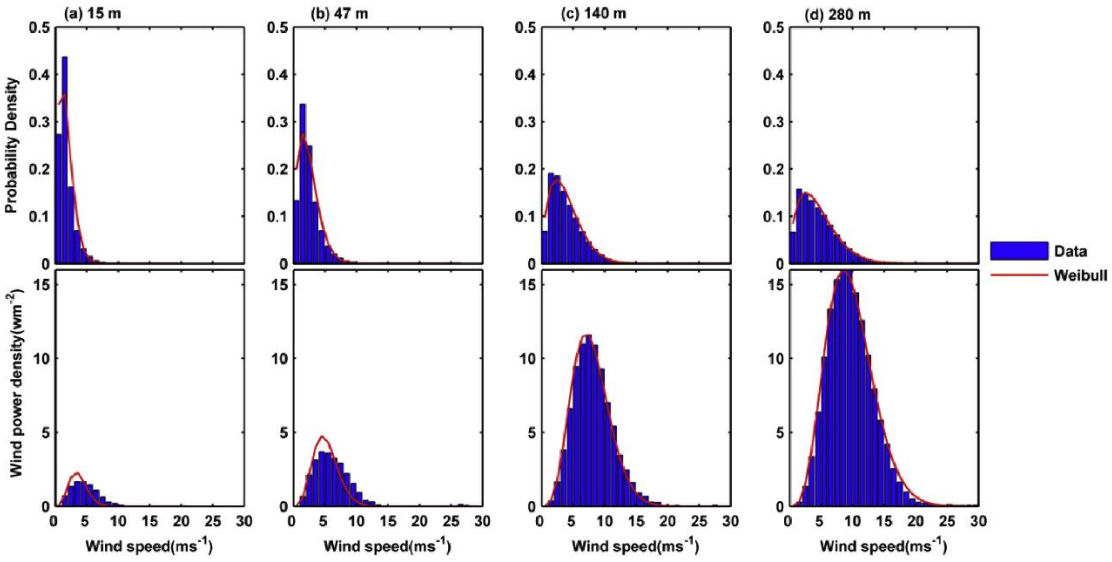

Fig. 4. The comparisons between Weibull function prediction and the wind data at four levels.

The contributions of different wind speed categories to wind power density are also illustrated in Fig. 4. Results show that the highest wind power density is produced in the smaller wind category with lower probability (15 m: wind speed of 3–4 m s^{-1} with a probability of 5%, 47 m: wind speed of 4–5 m s^{-1} with a probability of 8%, 140 m: wind speed of 7–8 m s^{-1} with a probability of 8%, and 280 m: wind speed of 8–9 m s^{-1} with a probability of 6%). Furthermore, even a small difference in higher wind speed in the probability density simulation can be magnified into a larger calculation error in wind power density (Table 2). Therefore, it is preferable to choose a model which can provide a satisfying estimation of the higher wind speeds than one that only does well in lower wind speed (Zhou et al., 2006). Generally, the Weibull

function is an efficient method in wind resource assessment at these levels, especially at the higher levels.

Table 2. The biases of probability density and wind power density (wm^{-2}) between Weibull function prediction and the measurements.

Height (m)	Probability density·10^{-4}			Wind power density·10^{-2}		
	0–3 m s^{-1}	3–6 m s^{-1}	>6 m s^{-1}	0–3 m s^{-1}	3–6 m s^{-1}	>6 m s^{-1}
15	533.7	97.3	5.5	22.2	41.7	16.7
47	446.5	158.5	5.4	4.5	87.6	41.4
140	200.8	64.9	3.3	3.6	56.7	28.1
280	118.2	54.3	3.4	5.5	44.5	18.3

3.4. Vertical distribution of wind resource

Currently, there are different sizes and heights of wind turbines in the wind energy market. Overall, the wind turbine size increases with height. In order to choose wind turbines with a reasonable size and make optimal use of wind resource safely, it is crucial to estimate the vertical variations of wind resource and wind shear first. Using the wind data at 15 levels of the meteorological tower, we analyzed the vertical distribution of the MWS, EWPD, and wind shear. As shown in Fig. 5, the MWS and EWPD increase with the height, and the distribution curves almost each present the logarithm and linear law. Also, the profiles of MWS consist of two logarithmic parts with different slopes, this is usually called the “kink” phenomenon due to the heterogeneity over urban terrain (Li et al., 2010). This phenomenon implies that the selections of parameters used in the interpolation method of log-law should consider the local representativeness, since only the parameters derived from the wind profile

below the “kink” can reflect the characteristics of surrounding underlying surface (Li et al., 2010). The seasonal variations at different levels are also similar to the results in Table 1, where the wind resource is greatest in spring and least in summer. According to the classification criteria of wind resource from Zheng et al. (2012), wind resource could be divided into poor areas, available areas, subrich areas, and rich areas. The annual MWS of 15 levels are below 5 m s-1 and the annual EWPD of 15 levels are greater than 40 wm−2. Although the MWS at 15 levels are relatively small, these levels still could be considered as available areas, since EWPD is the more important index. The maximum (minimum) values are at the highest (lowest) level, therefore, it seems that the highest level is the best installed height of wind turbine without considering other factors.

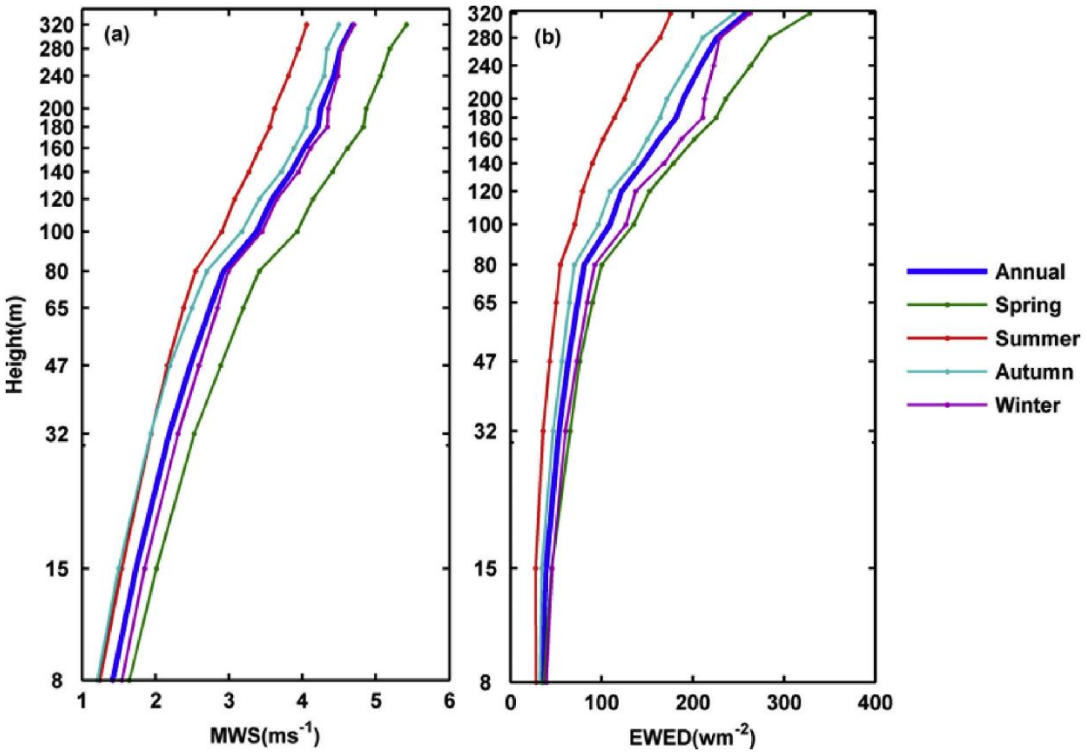

Fig. 5. The vertical distributions of (a) wind speed and (b) effective wind power density in log-law format.

As mentioned above, wind shear is an important factor affecting the safety of wind turbines. It increases and then decreases with height in Fig. 6, and it is especially strong at a height of 65–180 m. The initial increase starts at the height of 65–100 m and the initial decrease starts at the height of 100–140 m. Such behavior indicates that the strongest wind shear layer exists between 80 and 100 m, which provides a good match to the height of “kink” of nearly 80 m in Fig. 5a. The average wind shear of 0.31 in autumn is the highest, compared to the lowest value of 0.27 in winter. In conclusion, the better height is below 80 m considering its common installed height, and winter and spring are still the best seasons for exploiting wind resource at all levels.

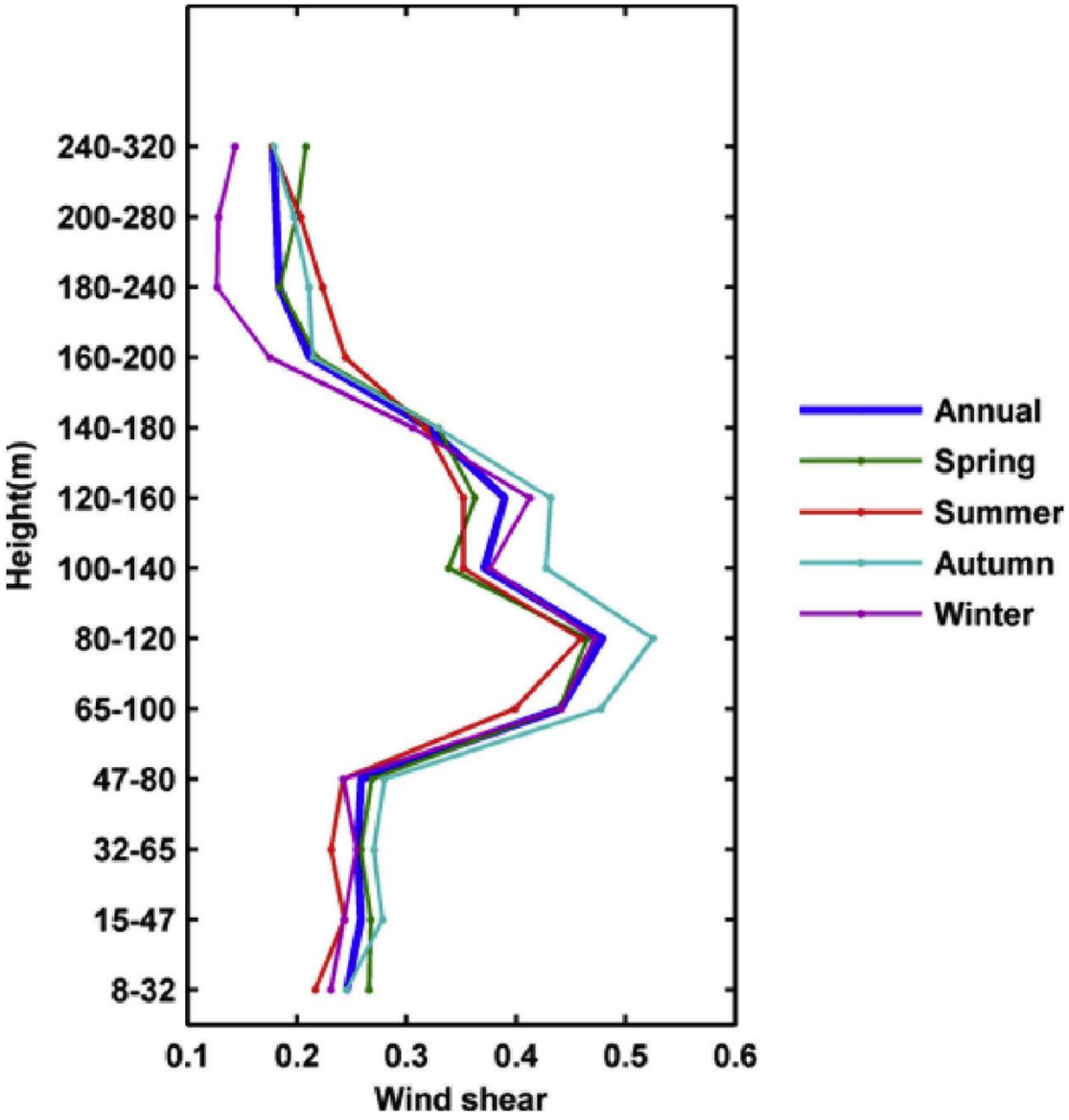

Fig. 6. The vertical distribution of wind shear in Beijing.

3.5. Spatial distribution of wind resource

Compared to the above analyses which focused on a single site, the construction of wind farm needs a large spatial scope of wind resource assessment. Therefore, based on data from the meteorological tower, the WAsP software was used to analyze spatial distribution of wind resource with high resolution (1 by 1 km). The 2 MW wind turbine (Performance curves in Fig. 7) in WAsP was used to estimate the annual electricity

production (AEP). The MWS, EWPD and AEP at the common installation height of 50 m are shown in Fig. 8.

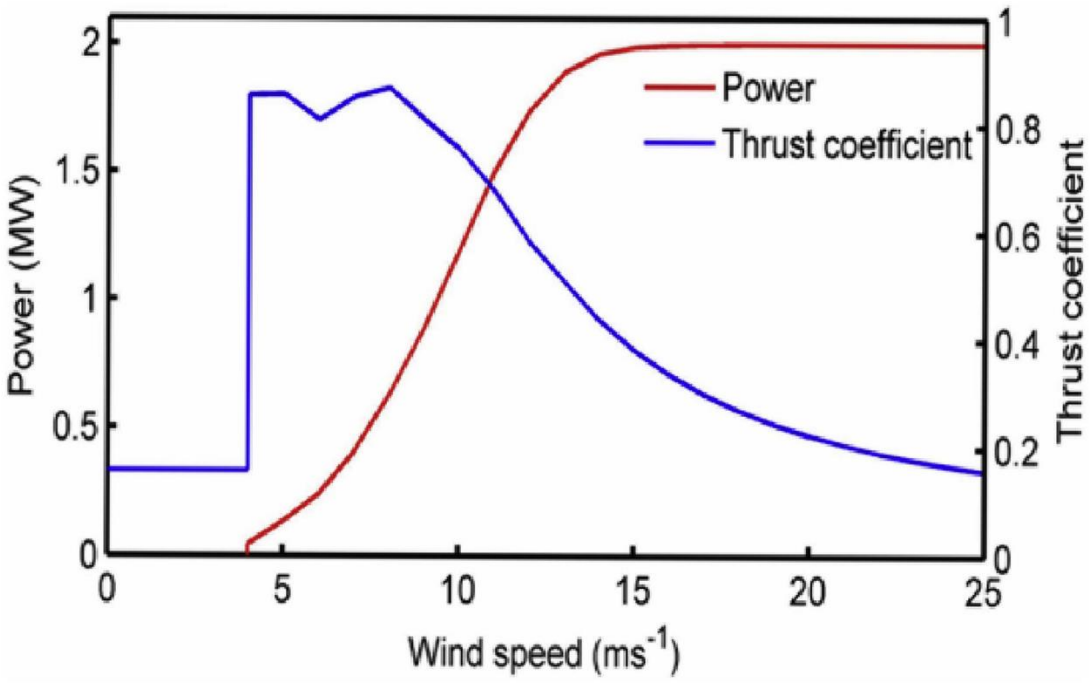

Fig. 7. The wind turbine performance curves.

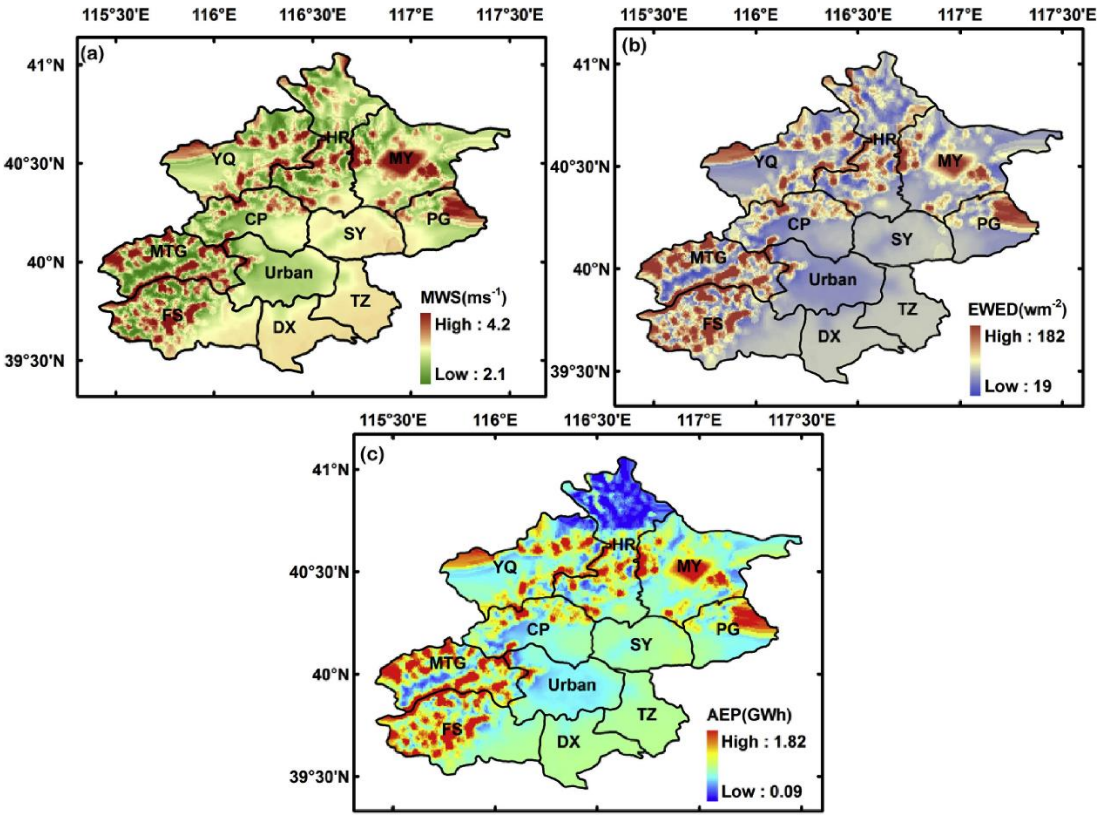

Fig. 8. The spatial distributions of (a) mean wind speed, (b) effective wind power density and (c) annual electricity production in Beijing.

In Fig. 8, the spatial differences of MWS, EWPD and AEP are distinct. The maximums of MWS, EWPD and AEP are 2 times, 10 times and 20 times higher than the minimums of MWS, EWPD and AEP. The large values usually occur in the mountains with higher terrain, while the small values occur on the plains with lower terrain. These findings suggest that the terrain has a large impact on MWS, EWPD and AEP. The more the elevation changes, the more wind resource there is. Additionally, the larger values are concentrated in northwestern or northern Beijing, which is consistent with the spatial distribution assessed by Zhang et al. (2014) in China with a 31-year dataset. Such pattern is due to the large topographic difference in the northwest or north zone, and it makes the mountain valley breeze more intense in this zone (Liu et al., 2009). The higher terrain located in windward slope could also weaken strong north wind in southern and eastern Beijing. Compared to wind resource in the urban area, the zones in suburbs such as MTG, FS, CP, MY and PG are more suitable for the development of wind resource. However, regardless of the uncertainties in WAsP, the regional averages of MWS, EWPD and AEP are 2.8 m s^{-1}, 55 wm^{-2} and 0.9 GW h. RenewableUK (2010) suggested that a typical onshore turbine of 1.8 MW may produce electricity by 4.7 GW h each year. In comparison, wind resource in Beijing is relatively deficient and is generally suitable for small wind turbines with small MWS and EWPD as recommended by RenewableUK.

3.6. Trend of wind resource

Under the pressure of climate change and air pollution, the exploitation of clean energy such as wind energy offers us an alternative way to solve these problems. In this section, Sen's slope method (Sen, 1968) was employed to determine the trends of MWS, EWPD. As shown in Fig. 9, the filled bar represents the level that pass 95% confidence level test. The negative trend rates at 15 levels demonstrate that the MWS and EWPD are decreasing. The range of trend rates of MWS is from 0.008 m $s^{-1}a^{-1}$ to 0.021 m $s^{-1}a^{-1}$, and that of EWPD is between 0.30 and 2.62 $wm^{-2}a^{-1}$. Vautard et al. (2010) pointed out that the weakening of large-scale circulation and an increase of surface roughness were the main reasons for wind speed decrease, which also could result in the reduction of wind energy (Zhou et al., 2006). In general, the reductions of wind resource at lower levels (below 100 m) are smaller than those at higher levels. The downtrend of wind resource is unfavorable to the sustainable exploitation of wind energy. On the contrary, the significant increasing trends of wind power density in East China Sea and South China Sea have been shown in Zheng et al. (2012), which are beneficial to the development and utilization of offshore wind energy. By analyzing outputs from the current generation of regional climate models, Pryor and Barthelmie (2011) further considered that the wind resource in regions of greatest wind energy would not move beyond the historical envelope of variability at least within the next 50 years. Their result implies that the trend variation of wind resource differs at different locations, and longer-term data of more sites in Beijing are required to further investigate whether wind resource in Beijing is decreasing.

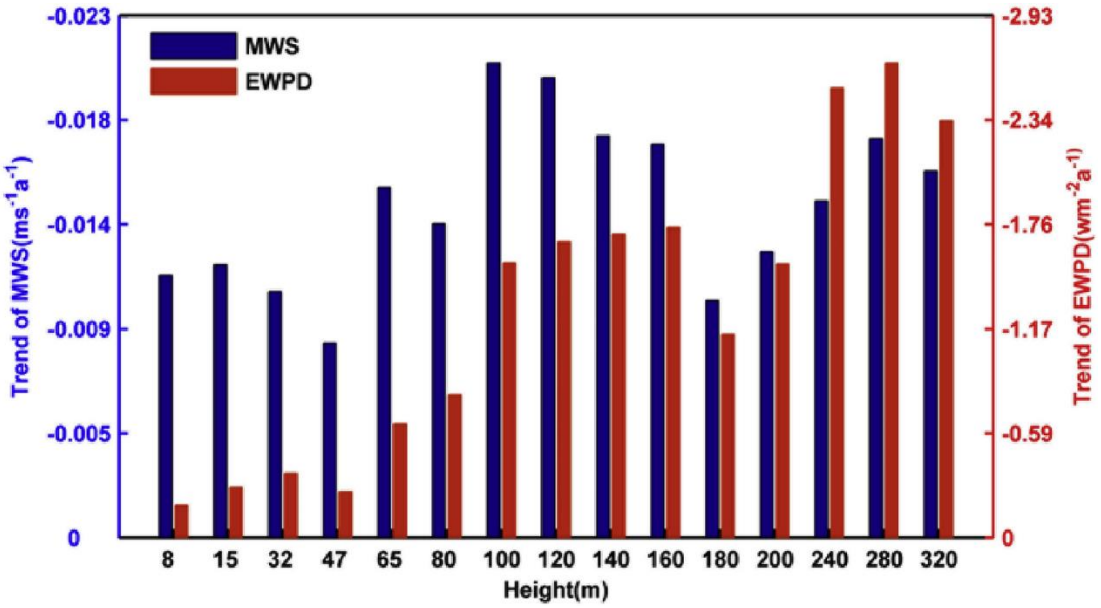

Fig. 9. The trend rates in wind resource from 1991 to 2011 at all levels over Beijing.

4. Conclusion and policy implication

Although the renewable energy market is huge in China, the exploitation of wind energy also needs to be considered comprehensively for practicality. The estimation of potential wind resource is a key step for the wind energy industry's development. We used the Weibull function and WAsP model for the wind data of 15 levels at a 325 m meteorological tower during 1991–2011 to conduct a case study in Beijing, and we drew the following conclusions.

In general, Weibull function can simulate the actual wind speed accurately, especially at higher levels. The highest wind power density is mainly produced by small wind category with smaller probability. However, this distribution function also needs to be improved for reducing the error in simulating wind power density at stronger wind categories and wind speed distribution at smaller wind categories at lower levels.

The annual and diurnal variations of wind resource are significant. Wind resources

at all levels are hightest in spring and lowest in summer. The diurnal variation pattern of wind resource changes with height, wind resources in the daytime are larger than those in the nighttime at lower levels, while inverse variations occur at higher levels. Therefore, wind turbines should operated at full capacity during these optimal times. Wind resource also varies with wind direction, the maximum wind resource often occurs in the NW sector due to the stronger prevailing northwest winter monsoon. We conclude that it is better to make wind turbines face towards NW sector. The vertical distribution of MWS presents increasing trends with logarithm law and the EWPD increases linearly. However, considering the stronger wind shear that occurs above urban complex underlying surface, the ideal installed height of wind turbines is below the height of wind shear layer.

As for the spatial distribution of wind resource, higher MWS, EWPD and AEP are located in the areas of high terrain in northwestern or northern Beijing. Therefore, compared to the urban area, MTG, FS and CP and other suburbs are better for exploiting wind resource. The vast spatial difference also suggests that it is better to choose a distributed layout for wind turbine farm, and Hebei province surrounding Beijing also should participate in Beijing's wind energy exploiting taking advantage of its cheap and vast land. The regional cooperative development is an important direction of wind energy industry. Overall, the regional averages of the MWS, EWPD and AEP are relatively small, which implies that wind resource in Beijing has a development potential of small wind turbines. However, under the background of atmospheric stilling, there are clear decreasing trends for MWS and EWPD at all levels, which seems

to be unfavorable for a sustainable exploitation of wind energy.

Potential wind energy assessment is just an estimation of actual wind resoure and the existence of over-estimation or under-estimation is unavoidable so far. Therefore, we chose long-term data to make the estimation be as close to actual wind resource as possible. However, the assessment is still just one of the crucial steps for wind energy development. Finding ways to efficiently and safely exploit wind energy remain to be the main challenges. Future works also should pay more attention to the interaction between these factors, such as econimic cost, wind turbine safety and environment harm, so that more reliable recommendations could be put forward. On this basis, the government will be able to make relevant policies to contribute to the increase of the clean energy percentage and to reduce CO2 emissions for green development.

Acknowledgments

This work was supported by grants from National Key Projects of Ministry of Science and Technology of China (2016YFC0203304), National Natural Science Foundation of China (41275022, 41475014 and 41405018), Natural Science Foundation of JiangSu Province (Youth Fund, BK20160957) and Major Project of the National Social Science Foundation of China (16ZDA047).

References

Albadi, M.H., El-Saadany, E.F., Albadi, H.A., 2009. Wind to power a new city in Oman. Energy 34 (10), 1579-1586.

Bahaj, A.S., Myers, L., James, P.A.B., 2007. Urban energy generation: influence of micro-wind turbine output on electricity consumption in buildings. Energy Build. 39, 154-165.

Battery and Energy Technologies (BET), 2004. Electricity demand. http://www.mpoweruk.com/electricity_demand. (Accessed 27 August 2016).

Bechrakis, D.A., Deane, J.P., McKeogh, E.J., 2004. Wind resource assessment of an area using short term data correlated to a long term data set. Sol. Energy 76, 725-732.

Belu, R., Koracin, D., 2009. Wind characteristics and wind energy potential in western Nevada. Renew. Energy 34, 2246-2251.

Boehme, T., Wallace, A.R., 2008. Hindcasting hourly wind power across Scotland based on met station data. Wind. Energy 11, 233-244.

Childs, C., 2004. Interpolating surfaces in ArcGIS spatial analyst. ArcUser 3235, 569. July-September.

DTU Wind Energy, 2016. Welcome to WAsP the Wind Atlas Analysis and Application Program. http://www.wasp.dk. (Accessed 27 July 2016).

Fagbenle, R.O., Katende, J., Ajayi, O.O., Okeniyi, J.O., 2011. Assessment of wind energy potential of two sites in North-East, Nigeria. Renew. Energy 36, 1277-1283.

Fang, H.F., 2014. Wind energy potential assessment for the offshore areas of Taiwan west coast and Penghu Archipelago. Renew. Energy 67, 237-241.

Grant, A., Johnstone, C., Kelly, N., 2008. Urban wind energy conversion: the potential of ducted turbines. Renew. Energy 33, 1157-1163.

International Energy Agency (IEA), 2011. World Energy Outlook 2011. Paris.

Ishugah, T.F., Li, Y., Wang, R.Z., Kiplagat, J.K., 2014. Advances in wind energy resource exploitation in urban environment: a review. Renew. Sust. Energy Rev. 37, 613-626.

Islam, M.R., Saidur, R., Rahim, N.A., 2011. Assessment of wind energy potentiality at Kudat and Labuan, Malaysia using Weibull distribution function. Energy 36, 985-992.

Jimenez, B., Durante, F., Lange, B., Kreutzer, T., Tambke, J., 2007. Offshore wind resource assessment with WAsP and MM5: comparative study for the German Bight. Wind. Energy 10, 121-134.

Keyhani, A., Ghasemi-Varnamkhasti, M., Khanali, M., Abbaszadeh, R., 2010. An assessment of wind energy potential as a power generation source in the capital of Iran, Tehran. Energy 35 (1), 188-201.

Ko, K., Kang, M., Huh, J., 2009. Year-to-year variation in wind resource and assessment of WAsP prediction for wind machine power. J. Mech. Sci. Technol. 23, 750-757.

Koroneos, C., Dompros, A., Roumbas, G., 2007. Renewable energy driven desalination systems modelling. J. Clean. Prod. 15 (5), 449-464.

Laiola, E., Giungato, P., 2017. Wind characterization in Taranto city as a basis for innovative sustainable urban development. J. Clean. Prod. https://doi.org/ 10.1016/j.jclepro 2017.05.111 in press.

Li, Q.S., Zhi, L.H., Hu, F., 2010. Boundary layer wind structure from observations on a 325 m tower. J. Wind. Eng. Ind. Aerod 98, 818-832.

Liu, S.H., Liu, Z.X., Li, J., Wang, Y.C., Ma, Y.J., Sheng, L., Liu, H.P., Liang, F.M., Xin,

G.J., Wang, J.H., 2009. Numerical simulation for the coupling effect of local atmospheric circulations over the area of Beijing, Tianjin and Hebei Province. Sci. China. Ser. D-Earth. Sci. 52, 382-392.

Liu, Y., Xiao, L.Y., Wang, H.F., Dai, S.T., Qi, Z.P., 2013. Analysis on the hourly spatio-temporal complementarities between China's solar and wind energy resources spreading in a wide area. Sci. China. Technol. S. C. 56, 683-692.

Martin, L., 2010. Wind energyethe facts: a guide to the Technology, economics and future of wind power. J. Clean. Prod. 18, 1122-1123.

Nfaoui, H., Buret, J., Sayigh, A.A.M., 1998. Wind characteristics and wind energy potential in Morocco. Sol. Energy 63, 51-60.

Oke, T.R., 1988. The urban energy-balance. Prog. Phys. Geogr. 12, 471-508.

Persaud, S., Flynn, D., Fox, B., 1999. Potential for wind generation on the Guyana coastlands. Renew. Energy 18, 175-189.

Pishgar-Komleh, S.H., Keyhani, A., Sefeedpari, P., 2015. Wind speed and power density analysis based on Weibull and Rayleigh distributions (a case study: firouzkooh county of Iran). Renew. Sust. Energy Rev. 42, 313-322.

Pryor, S.C., Barthelmie, R.J., 2011. Assessing climate change impacts on the near- term stability of the wind energy resource over the United States. PNAS 108, 8167e8171.

RenewableUK, 2010. Small Wind Systems. http://www.bwea.com/small/faq.html. (Accessed 27 August 2016).

Sen, P.K., 1968. Estimates of the regression coefficient based on Kendall's tau. J. Am. Stat. Assoc. 39, 1379-1389.

Stankovic, S., Campbell, N., Harries, A., 2009. Urban wind energy. Earthscan 122-125.

Sveinbjornsson, S., 2013. Analysis of WAsP (Wind Atlas Analysis and Application Program) in Complex Topographical Conditions Using Measured Production from a Large Scale Wind Farm. University of Washington [dissertation].

Truepower, A.W.S., 2010. Open Wind-theoretical Basis and Validation technical report 1.3. Albany, New York.

Vautard, R., Cattiaux, J., Yiou, P., The´paut, J.-N., Ciais, P., 2010. Northern Hemisphere atmospheric stilling partly attributed to an increase in surface roughness. Nat. Geosci. 3, 756-761.

Wang, L.L., Li, D., Gao, Z.Q., Guo, X.F., Bou-Zeid, E., 2014. Turbulent transport of momentum and scalars above an urban canopy. Bound-lay. Meteorol. 150, 485-511.

Wang, W.C., Teah, H.Y., 2017. Life cycle assessment of small-scale horizontal axis wind turbines in Taiwan. J. Clean. Prod. 141, 492-501.

Walker, S.L., 2011. Building mounted wind turbines and their suitability for the urban scale-A review of methods of estimating urban wind resource. Energy Build. 43, 1852-1862.

Wu, J., Wang, J.Z., Chi, D.Z., 2013. Wind energy potential assessment for the site of Inner Mongolia in China. Renew. Sust. Energy Rev. 21, 215-228.

Zeng, M., Zhan, K., Dong, J., 2013. Overall review of China's wind power industry: status quo, existing problems and perspective for future development. Renew. Sust. Energy Rev. 24, 379-386.

Zhang, D., Davidson, M., Gunturu, B., Zhang, X.L., Karplus, V.J., 2014. An Integrated

Assessment of China's Wind Energy Potential Report No. 261. London.

Zheng, C.W., Zhuang, H., Li, X., Li, X.Q., 2012. Wind energy and wave energy resources assessment in the East China Sea and South China Sea. Sci. China. Technol. S. C. 55, 163-173.

Zhou, W., Yang, H.X., Fang, Z.H., 2006. Wind power potential and characteristic analysis of the Pearl River Delta region, China. Renew. Energ 31, 739-753.

Zhou, Y., Wu, W.X., Liu, G.X., 2011. Assessment of onshore wind energy resource and wind generated electricity potential in Jiangsu, China. Energy Procedia 5, 418-422.